



Rare spatio-temporal interactions between conspecific species mingling and size inequality in a diverse Afromontane forest

Arne Pommerening^{a,*}, Graham Durrheim^b, Anna Mariager Behrend^c

^a Swedish University of Agricultural Sciences SLU, Faculty of Forest Sciences, Department of Forest Ecology and Management, Skogsmarksgränd 17, Umeå SE-901 83, Sweden

^b South African National Parks, Scientific Services, Rondevlei, PO Box 176, Sedgefield 6573, South Africa

^c Agricultural University of Iceland, Faculty of Environmental and Forest Sciences, Árleynir 22, Reykjavík 112, Iceland

ARTICLE INFO

Keywords:

Knysna Forest
Tree diversity
Mingling-size hypothesis
Janzen-Connell effects
Herd-immunity hypothesis
Mark cross correlation function
Voronoï/Dirichlet nearest neighbours

ABSTRACT

Spatial indices of tree diversity have often been proposed as surrogates of direct measures of biodiversity. They are comparatively straightforward to measure as part of forest ecosystem monitoring designed to alert to potentially negative effects of ongoing climate change. The loss of biodiversity, which is thought to be related to a decline in tree diversity, is perceived as a substantial threat, since biodiversity is also crucial to ecosystem resilience. We studied the correlation between community species mingling and size inequality of Knysna Forest, a well-known Afromontane forest ecosystem in South Africa, to better understand the principles of how nature maintains tree diversity. This is an important prerequisite for active conservation. The aforementioned correlation is indicative of the *mingling-size hypothesis* predicting that large trees are surrounded by significantly more heterospecific trees than smaller trees. The mingling-size hypothesis helps understand natural principles of tree diversity maintenance and is motivated by the well-known Janzen-Connell and herd-immunity hypotheses. Our results revealed that the correlation between spatial species mingling and size inequality is mostly negative at Knysna Forest, which is comparatively rare. This implies that the mingling-size hypothesis does not hold in this forest ecosystem. This has implications for conservation, because spatial size-inequality is no longer a by-product of high species mingling and potentially requires additional conservation effort. We could also show that the aforementioned negative correlation can be inferred from the mark cross correlation function when applying this spatial summary characteristic to the mingling and size inequality indices of individual trees.

1. Introduction

With ongoing climate change that is currently unfolding at a pace which is considerably faster than what we know from past events of natural climate change alterations, a widely perceived threat is a rapid loss of biodiversity (McElwee, 2021; Román-Palacios and Wiens, 2020). The potential loss of species is a serious concern in itself, however, research has also shown that biodiversity is crucial to ecosystem resilience and thus to sustaining terrestrial and marine ecosystems and habitats (Yachi and Loreau, 1999; Matias et al., 2013; Oliver et al., 2015; Fischer et al., 2006). The loss of biodiversity may therefore contribute to a destabilisation of ecosystems.

In this context, the continued monitoring of tree diversity is an efficient way to check on the rate of change in biodiversity in forest ecosystems, since tree diversity is closely correlated with more direct

measures of biodiversity (Pommerening and Grabarnik, 2019). Of particular interest are tree-diversity measures of spatial species mingling and size inequality (Gadow, 1993; Weiner and Solbrig, 1984), since these diversity components are the most important elements of spatial forest structure. Spatial species mingling describes the spatial interaction of tree species, i.e. how individual trees of certain species are spatially mixed with those of other species. Spatial size inequality or size diversity describes the spatial mixing of the sizes of individual trees, i.e. spatial tree size diversity. It is very common that mean species mingling and mean size inequality of the species populations in the same woodland are correlated (Wang et al., 2021). Interestingly, Pommerening and Uria-Diez (2017) and independently Wang et al. (2018) found that in many forest ecosystems there is a tendency for large trees to be surrounded by significantly more heterospecific trees than small and medium-sized trees and termed this observation the *mingling-size*

* Corresponding author.

E-mail address: arne.pommerening@slu.se (A. Pommerening).

<https://doi.org/10.1016/j.foreco.2024.121787>

Received 20 December 2023; Received in revised form 15 February 2024; Accepted 16 February 2024

Available online 29 February 2024

0378-1127/© 2024 The Author(s). Published by Elsevier B.V. This is an open access article under the CC BY license (<http://creativecommons.org/licenses/by/4.0/>).

hypothesis. The mingling-size hypothesis in turn can be motivated by the Janzen-Connell and the herd-immunity hypotheses (Janzen, 1970; Connell, 1971; Wills et al., 1997; Murphy et al., 2016) suggesting that natural competitors, herbivores and pathogens target conspecific plants in areas of high conspecific densities, eventually leaving only few specimens of a particular species alive. These specimens – in the absence of neighbouring trees, since they died – eventually develop into large trees whilst they are increasingly surrounded by much smaller trees from later colonisation cohorts. This combined effect of species and size replacement enforces both local size hierarchies (Ford, 1975; Suzuki et al., 2008) and the mingling of different tree species in a given area or patch, and naturally prevents the development of monocultures whilst facilitating tree diversity (Pommerening and Grabarnik, 2019).

A direct consequence of the mingling-size hypothesis is that mean species mingling and size inequality of species communities are positively correlated, i.e. where there is high species mingling in a given forest ecosystem, size inequality is high, too, and where species mingling is low so is size inequality. Conversely, in woodlands where negative correlation slopes occur this means that low species mingling can be found where there is high size differentiation and vice versa. The difference in sign of the slope of the linear relationship between community species mingling and size inequality indicates fundamentally different ecological patterns: Positive slopes stress the importance of between-species population size differences, because where heterospecific trees mingle their sizes are very different. Where negative slopes prevail, heterospecific trees often have similar sizes and size inequality is mainly a function of within-species size differences (Wang et al., 2021). In that case, the mingling size hypothesis does not hold and other ecological processes are at work that are not yet fully understood, since this pattern is rare. The correlation of species mingling and size inequality of species communities is therefore a valuable indicator of the mingling-size hypothesis which can easily be estimated from mapped tree data. Spatially explicit time series are still comparatively rare and the mingling-size hypothesis has so far been mostly studied in one-off monitoring plots.

The objectives of this paper are (1) to study the species community mingling-size inequality correlations of an Afromontane forest ecosystem, the Knysna Forest (South Africa), in time and space, (2) using point process statistics to identify underlying processes causing negative mingling-size inequality correlations and (3) based on our results to suggest options for active conservation in such forest ecosystems.

2. Materials and methods

2.1. Study data

The Knysna FVC monitoring area is part of the southernmost patches of the Afromontane forest in South Africa located south of the mountains between Humansdorp and Mossel Bay. The Knysna Forest represents the largest indigenous forest complex in South Africa. The monitoring area was established in the Diepwalle State Forest in 1937. The forest is located to the north of the southern coastal town of Knysna (at about 33° 57'S, 23° 11'E). Forest management experiments were carried out in the monitoring areas until 1954 and were completely abandoned at that time. This was followed by the initialisation of the Diepwalle forest dynamics monitoring project in the 1970s by scientists of the Saasveld Indigenous Forest Research Centre of the South African Forest Research Institute (Gadow et al., 2016). In 2005, the project and sites were transferred to the South African National Parks (SANParks) to become part of the Garden Route National Park.

The monitoring area used in this study is 380 m long and 120 m wide and involves 25 different species, most of them are of tropical origin. The most frequent species include ironwood (*Olea capensis* L. subsp. *macrocarpa*), kamassi (*Gonioma kamassi* E. MEY.) and real yellowwood (*Podocarpus latifolius* (THUNB.) R. BR. EX MIRB.). Knysna Forest is characterised by a rich variety of bryophytes, ferns, epiphytic lichens and orchids (Gadow et al., 2016). The study area is situated at 517 m a.s.

l and has a predominantly Southern aspect. The average annual maximum temperature for the region is 19.2 °C while the average minimum is 11.1 °C. Rainfall occurs in all seasons and the climate can be considered transitional between the tropical/subtropical and temperate regions. The mean annual precipitation may vary between 700 and 1230 mm, subject to orographic influences and is increasing from west to east (Gadow et al., 2016).

Full surveys of the FVC monitoring area were carried out in 1972, 1978, 1987, 1992 and 1997. All trees with a stem diameter (measured at 1.3 m above ground level) of at least 5 cm were included in the surveys, their stem diameters, spatial locations (in terms of Cartesian coordinates) were measured and the species were recorded. In between the survey years, birth and death processes occurred and were recorded as part of the survey work. We subdivided the elongated monitoring area into three large plots, plot 1, plot 2 and plot 3, with approximately the same size (130 × 120 m) to be able to distinguish between changes in both time and space, whilst maximising plot size so that there was a sufficiently large number of specimens per species at all survey times.

The summary characteristics quantified for each survey year and plot show many similarities (Table 1) with only slight differences: Plot 3 has markedly higher basal areas and number of trees per hectare than the other two plots. The stem diameter range is largest in plot 2. The quadratic mean diameter was highest in plot 1 throughout the survey years. Species mingling is much the same across all three plots, but highest in plot 1. Species richness is highest in plot 3 and stem-diameter differentiation is lowest in plot 3.

Seifert et al. (2014) analysed competition effects on stem-diameter growth and Gadow et al. (2016) studied the effects of tree species diversity and forest structure on tree growth and forest production at Knysna.

2.2. Tree diversity indices

In our study, spatial *species mingling* was quantified as the richness weighted species mingling index (Hui et al., 2008, 2011). Gadow (1993) defined spatial species mingling as the mean heterospecific fraction of plants among the k nearest neighbours of a subject plant i , i.e. $M_i = \frac{1}{k} \sum_{j=1}^k \mathbf{1}(\text{species}_i \neq \text{species}_j)$. Here, $\mathbf{1}(A)$ is an indicator function with $\mathbf{1}(A) = 1$, if A is true, otherwise $\mathbf{1}(A) = 0$. species_i denotes the species of subject tree i whilst species_j is the species of neighbour j . Hui et al. (2008, 2011) extended this concept of M_i by combining species mingling

Table 1

Basal area, G , number of trees per hectare, N , minimum stem diameter, d_{\min} , maximum stem diameter, d_{\max} , quadratic mean diameter, d_g , species mingling, \bar{M} , stem-diameter differentiation, \bar{T} , and global species richness, S , in the three Knysna plots.

Year	G [m ² ha ⁻¹]	N [ha ⁻¹]	d_{\min} [cm]	d_{\max} [cm]	d_g [cm]	\bar{M}	\bar{T}	S
Plot 1								
1972	25.2	549.4	5.5	66.7	24.2	0.57	0.42	20
1978	27.5	575.4	6.5	67.5	24.7	0.56	0.41	20
1987	31.0	641.7	6.9	70.4	24.8	0.57	0.41	20
1992	31.4	625.3	7.2	72.4	25.3	0.57	0.41	20
1997	32.0	631.5	7.3	72.2	25.4	0.58	0.40	20
Plot 2								
1972	24.6	574.9	5.8	73.5	23.4	0.55	0.41	21
1978	27.4	624.9	0.1	73.5	23.6	0.54	0.41	22
1987	30.2	685.6	6.7	74.6	23.7	0.57	0.40	22
1992	31.0	682.3	6.0	74.7	24.1	0.58	0.40	23
1997	31.5	680.3	6.8	75.3	24.3	0.57	0.39	23
Plot 3								
1972	29.0	717.3	6.3	71.7	22.7	0.55	0.38	22
1978	31.8	764.0	6.5	71.7	23.0	0.56	0.38	22
1987	35.8	821.2	6.4	73.3	23.5	0.55	0.39	23
1992	37.2	812.0	6.5	76.0	24.1	0.55	0.39	23
1997	37.7	808.0	6.5	74.7	24.4	0.56	0.39	23

with localised species richness (Eq. 1).

$$M_i = \frac{1}{k \times c} \sum_{j=1}^k \mathbf{1}(\text{species}_i \neq \text{species}_j) \times s_i \text{ with } c = \min(S, k + 1) \quad (1)$$

Accordingly, in Eq. (1) each M_i is multiplied by the local species richness s_i among the k nearest neighbours. Species richness is defined as the absolute number of species without reference to area (Magurran, 2004). Wang et al. (2021) amended the original index definition by introducing term c to ensure that the maximum number of species that are theoretically possible in a group of $k+1$ trees is limited by the number of species present in the forest stand or in the monitoring area studied. S is global species richness, i.e. the total number of species in a monitoring plot. Values of M_i are generally smaller and take a larger range of different values than those of M_i . All index values lie between 0 and 1.

Size inequality in this study was expressed as the mean ratio of smaller-sized and larger-sized stem diameters of the k nearest neighbours subtracted from one. Gadow (1993) referred to this diversity index as *size differentiation* (Eq. 2).

$$T_i = 1 - \frac{1}{k} \sum_{j=1}^k \frac{\min(d_i, d_j)}{\max(d_i, d_j)} \quad (2)$$

Here d_i denotes the stem diameter of subject tree i whilst d_j is the size of neighbour j . Size differentiation produces continuous results between 0 and 1 and T_i increases with increasing average size difference between neighbouring trees.

Readers interested in more details of spatial tree diversity indices are referred to the textbook by Pommerening and Grabarnik (2019).

2.3. Nearest neighbours and edge correction

There are many different neighbourhood concepts. In the past, neighbours were often identified by Euclidean distance, mainly for simplicity in field surveys and computations. Rajala and Illian (2012) pointed out that Euclidean neighbourhoods are *parametric*, since the number of nearest neighbours is a variable parameter and is often arbitrarily chosen (Pommerening and Grabarnik, 2019). In this study, we decided to base the tree diversity indices of Section 2.2 on *Voronoi*

neighbours which form *non-parametric* neighbourhoods (Rajala and Illian, 2012). Voronoi neighbours can be determined by Voronoi tessellation (also termed Dirichlet or Thiessen tessellation) which divides the entire plane into non-overlapping polygons with one tree location in each of them (Illian et al., 2008; Dale and Fortin, 2014). By definition, all pixels in each polygon are closer to the tree location of that particular polygon than to any other tree. Voronoi neighbours of a subject tree i are all those trees whose Voronoi polygon share a boundary with that of subject tree i (Fig. 1A). Voronoi neighbours better describe interactions from an individual-tree perspective, since the neighbourhood covers 360° around the subject tree. Rajala and Illian (2012) found that Voronoi neighbourhoods lead to more realistic estimations of spatial species mingling because they are less sensitive to the underlying point pattern formed by the tree locations.

As a result of tessellation, the trees have varying numbers k of nearest neighbours whilst with parametric neighbours, k is usually fixed. To our knowledge, this is the first time that Voronoi neighbours were used for an entire ecological study. In most other publications referenced in this article the number of nearest neighbours, k , has been set to a fixed, arbitrary value, e.g. $k = 4$.

For spatial edge correction we applied a variant of the nearest neighbour edge correction method referred to as NN2 by Pommerening and Stoyan (2006; Fig. 1B): All trees were excluded from the estimation of index population means whose polygons shared a boundary with the monitoring plots; however, such trees still served as Voronoi neighbours of others. This typically leads to an irregular buffer zone as shown in Fig. 1B. We used our own R code (R Development Core Team, 2023) and the R spatstat package (Baddeley et al., 2016) in these calculations.

2.4. Standardised major axis regression

As an alternative to simple linear regression we applied *standardised major axis* (SMA) regression, a method involving total least squares, where residuals are calculated with regard to both the x and the y axis (Warton et al., 2012). We applied SMA regression to the relationship between the arithmetic species population means of stem-diameter differentiation, \bar{T} , and species mingling, \bar{M} :

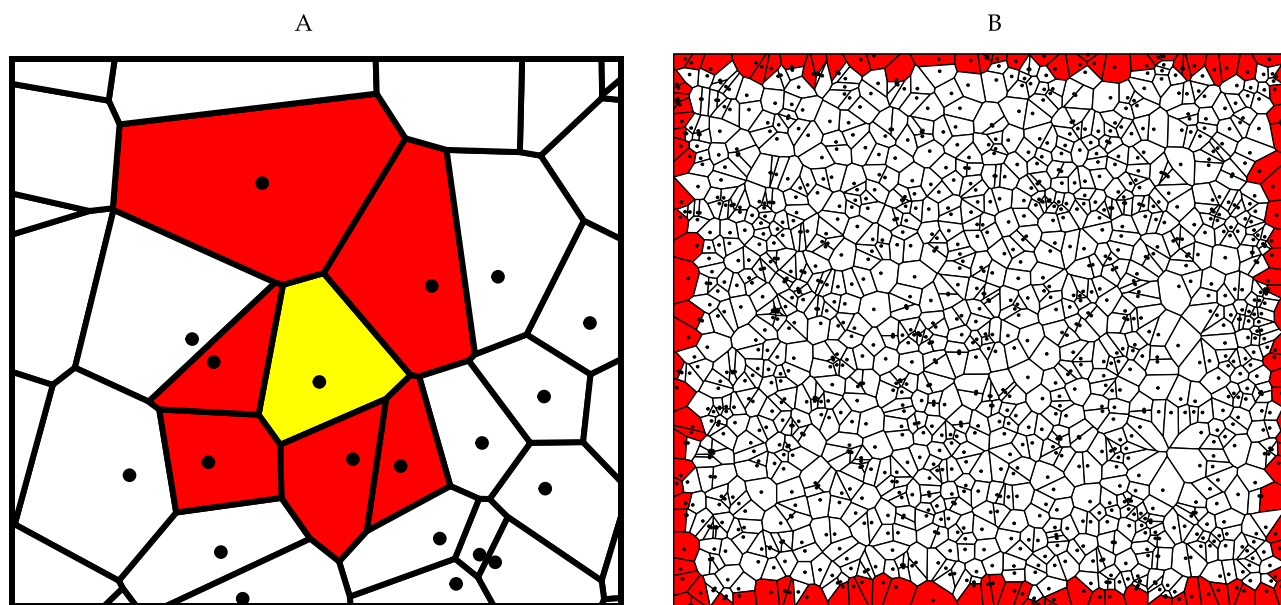


Fig. 1. A: The principle of Voronoi neighbourhoods: Voronoi neighbours (highlighted in red) are those that share a Voronoi polygon boundary with the polygon of the subject tree (highlighted in yellow). B: Voronoi tessellation of plot 3 (1992 survey; 130 × 117 m). The polygons that share a boundary with the plot boundary and are potentially affected by missing information on off-plot neighbours are highlighted in red. (For interpretation of the references to colour in this figure, the reader is referred to the web version of this article).

$$\bar{M} = a + b \times \bar{T} \quad (3)$$

Model coefficients a and b are the intercept (also termed elevation) and the slope of the linear model, respectively.

SMA regression has generally more in common with principal component analysis than with traditional linear regression and the method is highly recommended for studies of allometry (Pommerening et al., 2020) and plant traits. Since we were not interested in predicting one variable from another and there was no clear distinction between dependent and independent variables, estimating the intercept and slope was not a simple linear regression problem in our study. Besides simple linear regression often underestimates slope parameters b (Warton et al., 2006).

In order to quantify meaningful relationships between species population means of differentiation and mingling, we included only those species that had more than 18 specimens in a given plot. We carried out SMA regressions and associated tests using the R `smatr` package (Warton et al., 2012).

Past analyses using many different data sets from across the world have revealed that the slopes involved in the linear relationship $\bar{M} \sim \bar{T}$ are usually positive (Pommerening and Uria-Diez, 2017; Wang et al., 2021).

2.5. Mark correlation functions and mark cross correlation functions

The *mark correlation function* $k_{mm}(r)$ is a second-order characteristic assessing the similarity and dissimilarity of marks at given distances r (Penttinen et al., 1992; Stoyan and Penttinen, 2000; Illian et al., 2008; Pommerening and Grabarnik, 2019). In the mark correlation function, the product of the marks of a pair of trees is calculated at distance r between them. From the single values for each pair of trees a mean is computed for each r . Thus, the function $k_{mm}(r)$ is conceived, which is dependent on r . It is advisable to divide the function by the square of the mean mark, \bar{m}^2 , in order to make interpretation easier. Illian et al. (2008) gave the estimator of the mark correlation function as

$$\hat{k}_{mm}(r) = \frac{1}{\bar{m}^2} \sum_{\xi_i, \xi_j \in W}^{\neq} \frac{m(\xi_i) m(\xi_j) k_h(\|\xi_i - \xi_j\| - r)}{2\pi r A(W_{\xi_i} \cap W_{\xi_j})}. \quad (4)$$

Here, ξ_i and ξ_j are arbitrary tree locations in the forest monitoring plot W . $m(\xi_i)$ and $m(\xi_j)$ are so-called marks, i.e. additional information on the trees, e.g. stem diameters or total heights of the trees at locations ξ_i and ξ_j . However, in our study we used the individual tree species mingling and stem-diameter differentiation indices M_i (Eq. 1) and T_i (Eq. 2) as marks. k_h in our case is the Epanechnikov kernel function, a function dealing with pairs of trees that approximately have distance r between them but whose inter-tree distance slightly differs from r . $A(W_{\xi_i} \cap W_{\xi_j})$ is the area of intersection of W_{ξ_i} and W_{ξ_j} , see Illian et al. (2008, p. 481 f. and p. 188), relating to the translation edge correction (Ohser and Stoyan, 1981).

When trees at close proximity both have small marks, this typically causes mark correlation functions to be smaller than 1. For $k_{mm}(r) > 1$ both trees of pairs at close proximity need to have marks larger than the mean mark. With $r \rightarrow \infty$ the mark correlation function tends towards the limit of 1 indicating situations where there is no spatial correlation between the marks at distance r . The actual limit may, however, differ from 1 because of statistical fluctuations and spatial inhomogeneity (Ballani et al., 2019).

In the context of this study, where we are interested in the relationship between species mingling and stem-diameter differentiation, it makes sense to consider the *mark cross correlation function* (Stoyan, 1987) in addition to the mark correlation functions and to apply it to the mingling and differentiation marks. The mark cross correlation function $k_{lm}(r)$ simultaneously considers two quantitative marks characterising every point (i.e. tree location) of a given spatial tree pattern and

addresses the question, which spatial correlations exist between the two marks. In analogy to Eq. (4) and following Stoyan (1987), we can write the estimator of the mark cross correlation function as

$$\hat{k}_{lm}(r) = \frac{1}{\bar{l}\bar{m}} \sum_{\xi_i, \xi_j \in W}^{\neq} \frac{l(\xi_i) m(\xi_j) k_h(\|\xi_i - \xi_j\| - r)}{2\pi r A(W_{\xi_i} \cap W_{\xi_j})}. \quad (5)$$

The notation is the same as for Eq. (4), however, two different types of quantitative marks are considered now, i.e. $l(\xi_i)$ and $m(\xi_j)$. In our application, $l(\xi_i)$ and $m(\xi_j)$ are defined by M_i (Eq. 1) and T_i (Eq. 2). The interpretation of $k_{lm}(r)$ largely follows that of $k_{mm}(r)$: When trees at close proximity both have small species mingling and size differentiation index values this typically causes the mark cross correlation functions to be smaller than 1 and indicates positive correlation. For $k_{lm}(r) > 1$ both trees at close proximity need to have diversity indices larger than the mean mark. This would also lead to a positive correlation of the two index marks. With largely different values of M_i (Eq. 1) and T_i (Eq. 2) trees at close proximity and with $r \rightarrow \infty$ the mark cross correlation function tends towards the limit of 1 indicating situations where there is no spatial correlation between M_i and T_i at distance r .

For each forest plot and survey year we estimated $k_{mm}(r)$ twice, once where all quantitative marks were M_i and once where T_i was the exclusive mark. Finally we estimated $k_{lm}(r)$ for both marks simultaneously.

In our study we used pointwise envelopes for testing the $k_{lm}(r)$ functions. This procedure was based on 999 simulations of spatial tree patterns where the locations were fixed while the two M_i and T_i marks were permuted, i.e. the indices were independently and randomly re-assigned to the trees. The simulated patterns obtained by this procedure follow the so-called *random labelling hypothesis* (Illian et al., 2008). Statistical inference is then based on a visual comparison of observed and simulated functions which were summarised by pointwise 95% envelopes. If the behaviour of the observed functions is not typical of random labelling, i.e. if the corresponding curves are located outside the envelopes, we concluded that there may be ecological reasons to expect that the diversity indices of close trees are significantly related to each other (Pommerening and Grabarnik, 2019).

When plotting the graphs of the two $k_{mm}(r)$ functions and of $k_{lm}(r)$ and studying them, it is visually evident that the graph of the mark cross correlation function is influenced by both mark correlation functions (Stoyan, 1987). Usually the influence of one $k_{mm}(r)$ function appears to be stronger than that of the other one which can be gauged from the proximity of the two graphs to that of $k_{lm}(r)$. Consequently a distance measure was necessary to determine the proximity of the two $k_{mm}(r)$ functions to the corresponding $k_{lm}(r)$ function. For deriving such a distance measure we modified an approach taken by Pommerening et al. (2011) and calculated the sum of the absolute differences between $k_{mm}(r)$ and of $k_{lm}(r)$ using a step width of 0.25 m between minimum distance, r_0 , and an upper limit $r_1 = 30$ m:

$$\Delta_m = \sum_{r_0}^{r_1} |k_{mm}(r) - k_{lm}(r)| \quad (6)$$

The upper limit r_1 was chosen so that it approximately corresponded with the maximum correlation range of the mark (cross) correlation functions but also considered the size of the monitoring plot at the same time. For each plot and survey year, Δ_m was calculated twice, i.e. once for $k_{mm}(r)$ using M_i and once for $k_{mm}(r)$ using T_i as marks. This resulted in two deviation measures, Δ_M and Δ_T . Finally, we calculated the deviation ratio Δ as

$$\Delta = \frac{\Delta_T}{\Delta_M}. \quad (7)$$

The smaller Δ , the larger is the influence of $k_{mm}(r)$ (using only T_i as marks) on $k_{lm}(r)$ and the smaller is the influence of $k_{mm}(r)$ based entirely on M_i marks. For $\Delta = 1$, the influence of both mark correlation functions

on $k_{lm}(r)$ would be the same and for $\Delta > 1$ the influence of $k_{mm}(r)$ solely based on M_i is greater than that of $k_{mm}(r)$ using T_i marks only. The mark (cross) correlation functions were calculated using the R `spatstat` package (Baddeley et al., 2016).

3. Results

Examining the relationship between individual-tree species mingling M_i and size differentiation T_i revealed quite similar, seemingly uninteresting patterns throughout the three plots and the five survey periods (Fig. 2) when inspected superficially. The main differences occur at the fringes of the main data clouds, i.e. with very small and large T_i values.

For example, in plot 3 individual data points on the left-hand side of the main data clouds seem to disappear with time whilst more appear on the right-hand side where T_i values are large. There is also some variability, particularly between plots, i.e. in space, at the bottom of the data clouds where M_i values are low (Fig. 2). These differences at the peripheries of the main data cloud are likely to be the unique signatures of individual trees in space and time. Fig. 2 also highlights that the size differentiation values vary much more than those of species mingling, although the definition of Eq. (1) and the use of Voronoi neighbours with variable k increase the range of possible individual-tree mingling results compared to the traditional species mingling index with fixed k : For one and the same M_i value many different T_i can be observed. The range of T_i values is usually widest around $M_i = 0.5$, thus indicating the maximum width of the data clouds.

Our analyses have shown that the linear relationships $\bar{M} \sim \bar{T}$ (Section 2.4), i.e. the relationship of the means of the two diversity indices in each species community, are more similar in time than they are in space (Fig. 3). We can clearly see that between survey years intercept and slope vary only marginally, particularly in plot 3 (Fig. 3C), which was confirmed by the SMA tests for common slope and intercept (not shown). The greatest difference exists between the $\bar{M} \sim \bar{T}$ relationships of plots 1 and 3 (Fig. 3A and C) on one hand and that of plot 2 (Fig. 3B) on the other.

The Knysna FVC monitoring area is one of the few exceptions across the world where negative slopes in the $\bar{M} \sim \bar{T}$ relationship occur and prevail, namely in plots 1 and 3 (Fig. 3A and C). Here the negative sign of the slope is mainly driven by within-species population size differences. However, the $\bar{M} \sim \bar{T}$ relationship in plot 2 (Fig. 3B) follows the common, more frequent pattern where the positive sign is mainly caused by between-species population size differences (see Section 1).

The aforementioned similarities of the $\bar{M} \sim \bar{T}$ relationship in time are also confirmed by Fig. 4. Both intercepts (Fig. 4A) and slopes (Fig. 4B) are nearly horizontal lines over time, thus indicating little change. Also here, it is evident that plots 1 and 3 are similar in terms of both linear model coefficients whilst those related to plot 2 are quite different.

In general, the mark (cross) correlation functions did not differ much from the horizontal line through 1 indicating that the corresponding marks are not spatially correlated (Fig. 5), which may have been caused by differences in the index values of paired trees. Still, the 95% pointwise envelopes produced from 999 random labelling simulations clearly show that most of these functions indicate significant patterns particularly at short distances, but often also at larger distances, especially in plot 2, where it is possible that spatial inhomogeneities exist, e.g. gradual differences in tree density. The difference between the mark (cross) correlation functions and the horizontal line through 1 is particularly small for plot 3 across all survey years. In plot 1, the mark cross correlation function is significant between $r = 5 - 25$ m in 1972 and 1978. After that function $k_{lm}(r)$ is not significant anymore. The general shape of the function in plot 1 suggests comparatively large values of the two diversity indices at very short distances followed by

pairs of trees with indices of similar, but small size in the medium range and no correlation at very large r . In plot 2, the mark cross correlation function is significant after the first three metres and continues to be so up to $r = 50$ m and beyond throughout all survey years. The more or less constant deviation of $k_{lm}(r)$ from the horizontal line through 1 may indicate inhomogeneous spatial patterns. On the other hand it is very likely that this deviation indicates strong positive correlation between the two index marks caused by small values of M_i and T_i of the corresponding pairs of trees considered. This would support the positive correlations between $\bar{M} \sim \bar{T}$ shown in Fig. 3B. The general shape of the $k_{lm}(r)$ function in plot 2 suggests similar-sized large index values at short range followed by indices of similar, but small size throughout the remaining r range. In plot 3, only the first 8 m of the mark cross correlation function are outside the 95% pointwise envelopes, i.e. here short-range interactions between species mingling and size inequality are of particular interest. In this distance range, both diversity indices are similar, but small. For $r > 8$ m, $k_{lm}(r)$ in plot 3 mostly shows indices of paired trees with different values. Generally, the fact that the $k_{lm}(r)$ curves in plots 1 and 3 run more closely along the horizontal line through 1 supports the negative correlations between $\bar{M} \sim \bar{T}$ shown in Fig. 3A and C.

Possible answers to the question which of the two mark correlation functions, $k_{mm}(r)$, have a greater influence on and show a shorter distance to the graph of $k_{lm}(r)$ are supported by the results for Δ in Fig. 5. In plot 1, deviation Δ initially takes a value close to 1 where the influence of both $k_{mm}(r)$ over the first 30 m is similar. The value of Δ subsequently decreases over the years so that the influence of $k_{mm}(r)$ based entirely on differentiation (T_i) marks increases. A different trend unfolds in plot 2 where the initial $\Delta = 0.878$ steadily increases over the years to reach a maximum of $\Delta = 1.194$ in 1987. Δ values larger than 1 indicate an influence of $k_{mm}(r)$ (based on M_i marks) on $k_{lm}(r)$ which is stronger than that of $k_{mm}(r)$ using only differentiation marks. In plot 3, Δ takes the lowest value of all three plots indicating a strong relative influence of $k_{mm}(r)$ based entirely on differentiation marks on $k_{lm}(r)$. With the notable exception of 1978, where the value of Δ drops down to 0.494, in plot 3 deviation ratio Δ remains fairly constant throughout the survey years.

The final step of our analysis involved studying the relationship between deviation ratios Δ and slopes b of the 15 $\bar{M} \sim \bar{T}$ relationships. Here we analysed both spatial and temporal trends. The spatial trend can be observed between the three plots and the temporal trend describes the relationship within the plots over the survey years. According to the spatial trend, with increasing deviation ratio Δ the slope of the $\bar{M} \sim \bar{T}$ relationship increases exponentially (Fig. 6, grey curve). At approximately $\Delta = 1.032$ the slope changes signs from negative to positive. This is close to $\Delta = 1.0$ where the influence of both $k_{mm}(r)$ functions on $k_{lm}(r)$ is the same. According to the spatial trend, slope b turns from negative to positive exactly when the influence on $k_{lm}(r)$ exerted by $k_{mm}(r)$ based on mingling marks becomes stronger than $k_{mm}(r)$ using only differentiation marks.

The temporal trend within the three plots clearly differs from the exponential spatial trend. Separate temporal trends are obvious in Fig. 6, since the points relating to each of the three plots form distinctive, individual data clouds. Within each cloud we found linear relationships indicating that with increasing deviation ratio Δ the slope of the $\bar{M} \sim \bar{T}$ relationship decreases. Judging by the slopes, this temporal trend is stronger in plots 1 and 3 than in plot 2.

4. Discussion

In times of climate change, maintaining tree diversity is more important than ever for mitigating the loss of diversity and resilience in forest ecosystems (The Royal Society and the US National Academy of Sciences, 2020; McElwee, 2021; Román-Palacios and Wiens, 2020;

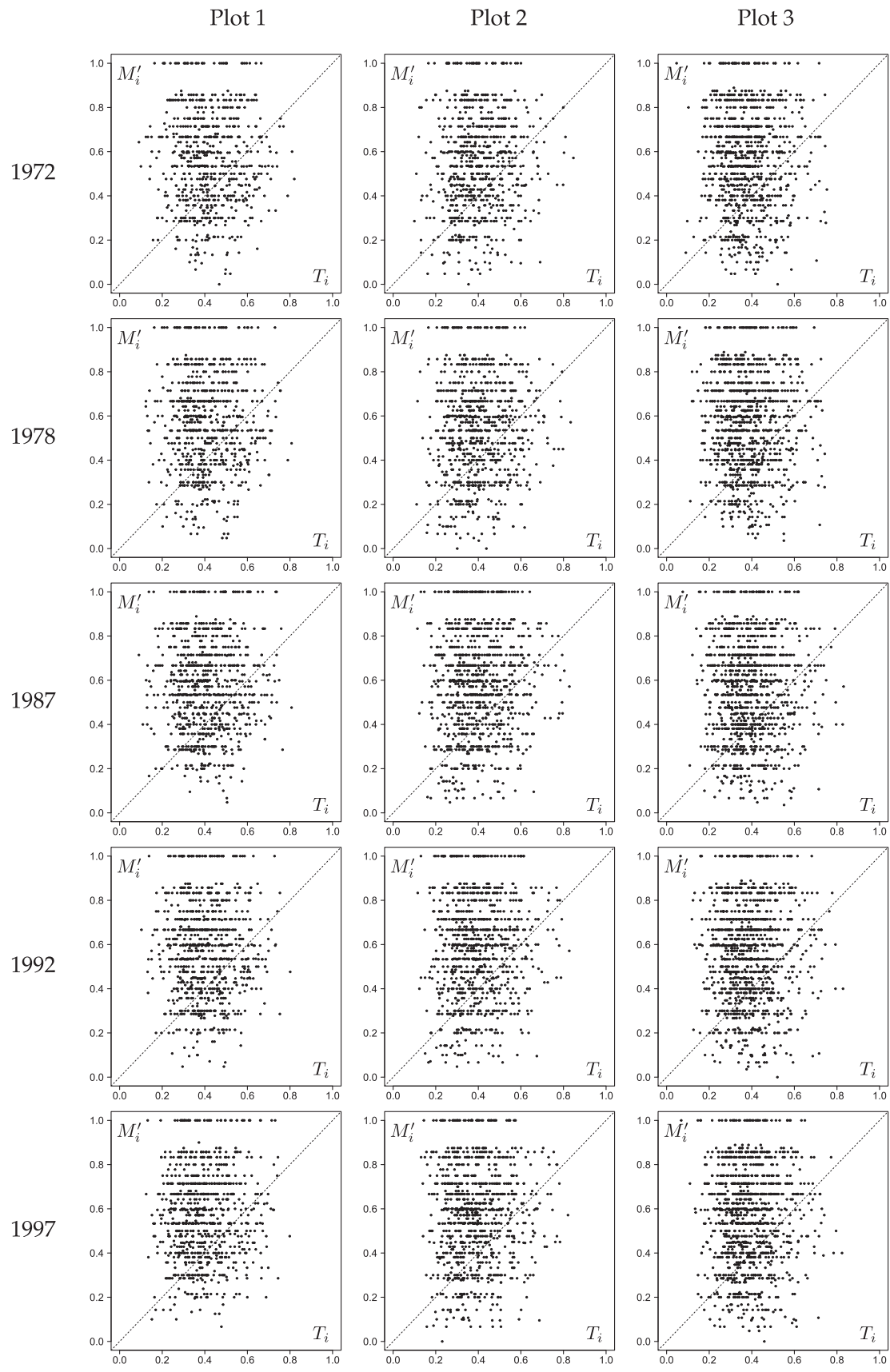


Fig. 2. Scatterplots of individual-tree species mingling, M'_i (Eq. 1), and size differentiation, T_i (Eq. 2), indices in the three plots and five survey years.

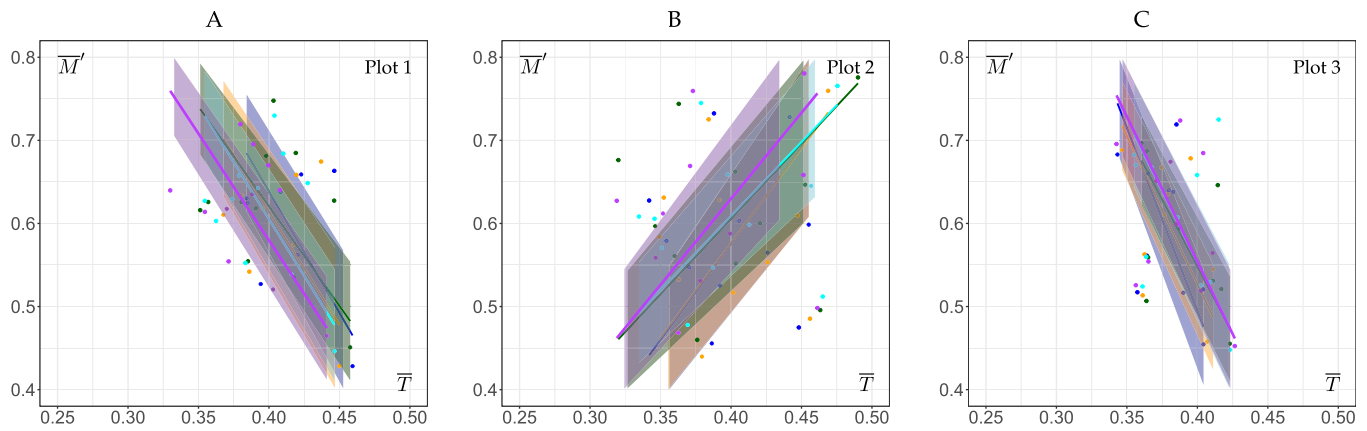


Fig. 3. Linear relationships $\bar{M}' = a + b \times \bar{T}$ (Eq. 3) between mean species mingling, \bar{M}' , and mean size differentiation, \bar{T} , of all tree species communities with more than 18 specimens per plot and obtained from standardised major axis (SMA) linear regression. A: plot 1. B: plot 2. C: plot 3. Blue: 1972, orange: 1978, green: 1987, cyan: 1992, purple: 1997. (For interpretation of the references to colour in this figure, the reader is referred to the web version of this article).

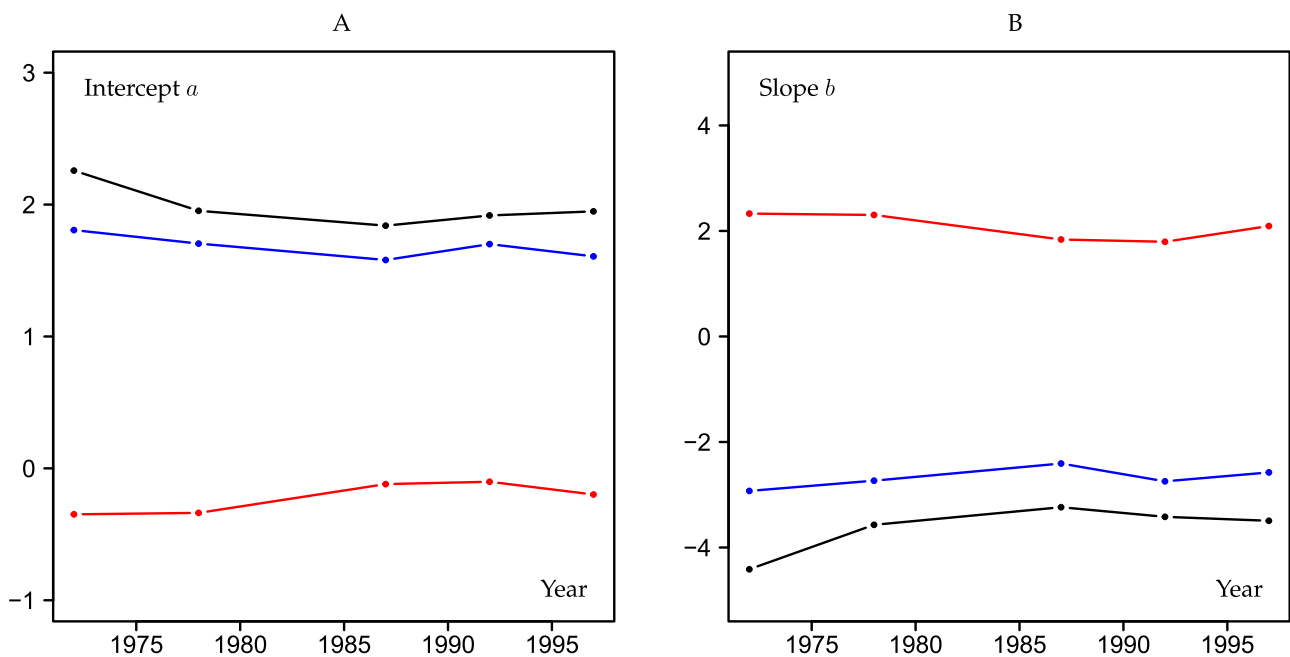


Fig. 4. Intercept (a , A) and slope (b , B) of the linear relationships $\bar{M}' = a + b \times \bar{T}$ (Eq. 3) between mean species mingling, \bar{M}' , and mean size differentiation, \bar{T} , across survey years. Blue: plot 1, red: plot 2, black: plot 3. (For interpretation of the references to colour in this figure, the reader is referred to the web version of this article).

Oliver et al., 2015; Fischer et al., 2006; Kühn et al., 2020; Hoffmann, 2022). A prerequisite for conservation and maintenance of tree diversity is a proper understanding of the mechanisms and processes in natural forest ecosystems. Accordingly, our study has made an effort to understand how spatial species mingling and size inequality are related in a key natural Afromontane forest ecosystem through time and space. These forest ecosystems are special, since they are small remnants of what originally were much larger natural forests and include a high diversity of tree species and sizes. They are also special with regard to the correlations between mean community spatial species mingling and size inequality which often have a negative sign. Ecologically, negative signs of this correlation imply that the corresponding size inequality is low whilst species community mingling is high and vice versa. In such situations the different species communities involved have similar size structures and size inequality is mainly the result of size diversity within the same species communities. This pattern is rare and does not often occur in forest ecosystems of different climate zones around the world

(Pommerening and Uria-Diez, 2017; Wang et al., 2021).

Our results have shown that the community correlation relationship $\bar{M}' \sim \bar{T}$ in the Knysna Forest plots does not change much with time, although the monitoring spans a time period of 25 years (Figs. 3 and 4). On first sight, this may seem a fairly short time for a tree-dominated plant community, however, given the climate eco-physiological processes are fast in such woodlands and spatially explicit time series data from such large research plots like those in the Knysna Forest are hard to come by. Our finding is consistent with earlier research that could demonstrate that spatial forest structure usually tends to differ more in space than in time (LeMay et al., 2009). The mark (cross) correlation functions applied to the individual-tree M'_i and T_i indices (Fig. 5) confirmed the same relative constancy of spatial forest structure in time. Ecologically this means that the spatial structure of the subtropical forest ecosystem at Knysna is comparatively resilient and well adapted to local sites.

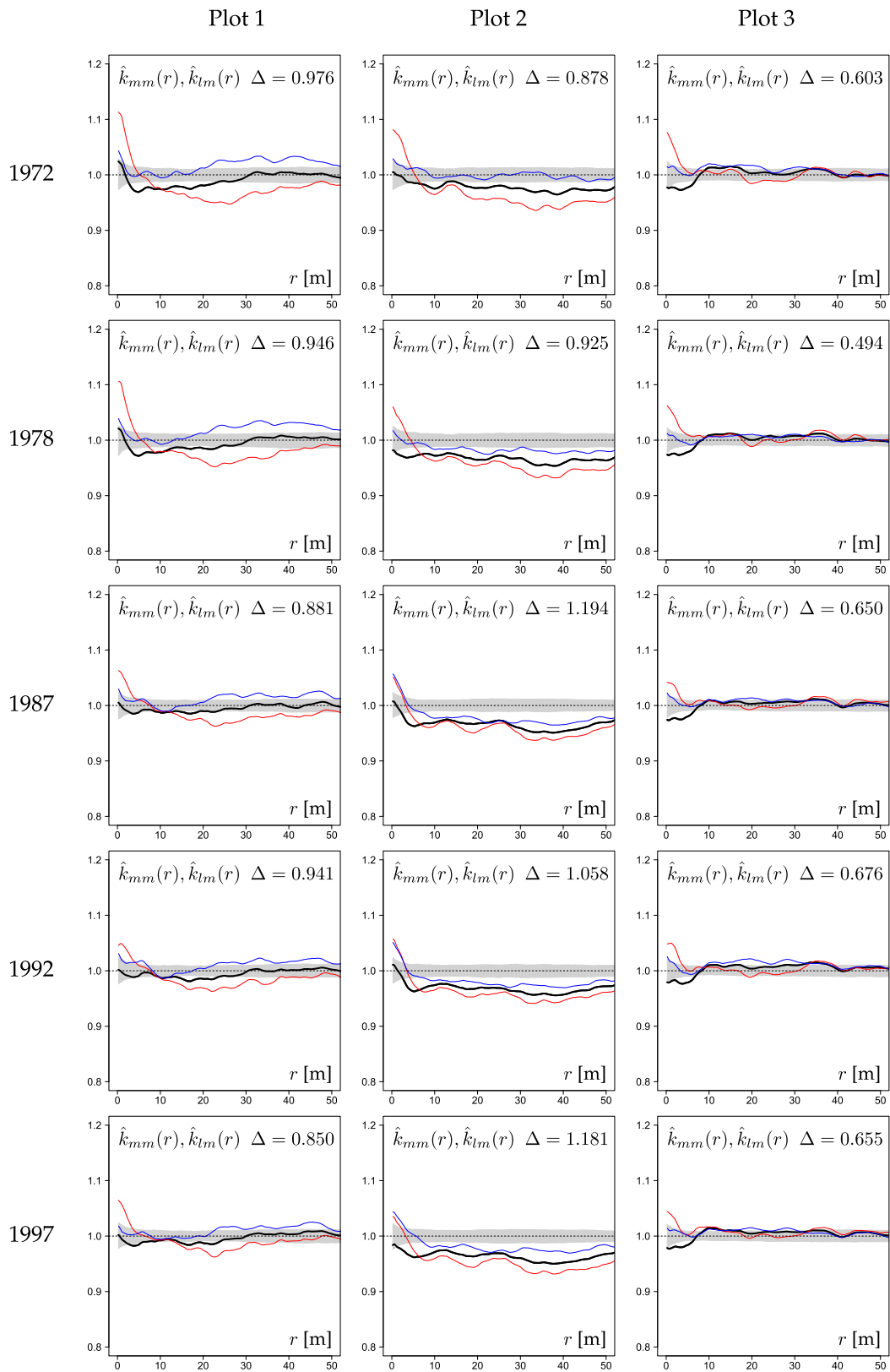


Fig. 5. Mark correlation functions $k_{mm}(r)$ based on either only M_i (Eq. 1) marks (red) or T_i (Eq. 2) marks (blue) and the mark cross correlation function $k_{lm}(r)$ using both marks simultaneously (black). The bandwidth parameter used in the estimation of both $k_{mm}(r)$ and $k_{lm}(r)$ was $h = 1.35$ m. The pointwise 95% envelopes calculated from 999 random-labelling simulations are shown in grey. The deviation measure Δ quantifies the relative influence of the two $k_{mm}(r)$ functions on $k_{lm}(r)$ and is defined in Eq. (7). The inter-tree distance is denoted by r . (For interpretation of the references to colour in this figure, the reader is referred to the web version of this article).

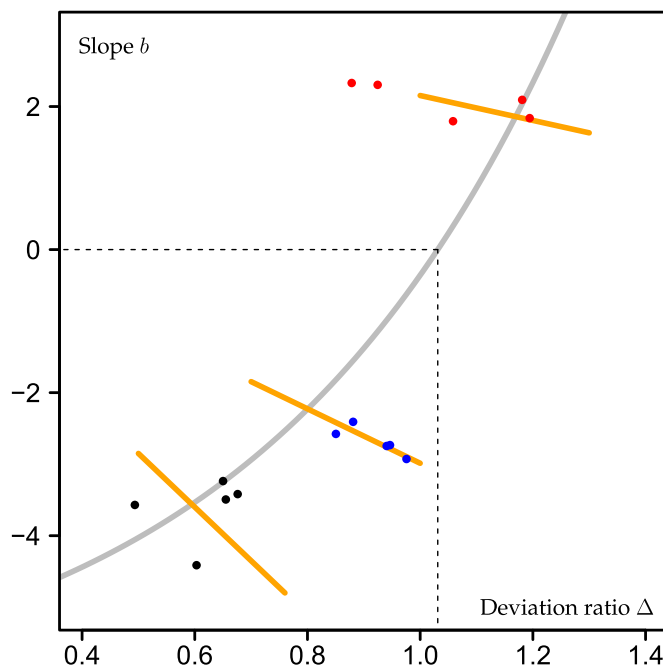


Fig. 6. The spatio-temporal relationship between slope b of the relationship $\bar{M} = a + b \times \bar{T}$ (Eq. 3) and the deviation measure Δ . The plot affiliation of the data is indicated by different colours (blue: plot 1; red: plot 2; black: plot 3). The spatial trend line (grey) is determined by the model equation $b = m + e^{a \times \Delta}$ ($R^2 = 0.53$). The dashed black lines indicate that slope b according to the spatial trend changes signs at $\Delta = 1.032$. The temporal trend lines (orange) are simple linear relationships. (For interpretation of the references to colour in this figure, the reader is referred to the web version of this article).

We applied the mark (cross) correlation functions to the spatial tree patterns of Knysna Forest in order to learn more about the individual-tree correlations between the M_i and T_i indices. These correlations differed between plots, however, the most interesting finding of our study was that the relative proximity of the two $k_{mm}(r)$ functions to the $k_{lm}(r)$ function expressed as quantity Δ is correlated with the slope of the $\bar{M} \sim \bar{T}$ species community relationship. Relative proximity of graphs is an expression of influence on the $k_{lm}(r)$ function and thus the relative importance of single-type marks, either M_i or T_i , motivate the type of influence (Stoyan, 1987). Our study highlighted that values of $\Delta < 1$ are typical of negative slopes of the $\bar{M} \sim \bar{T}$ relationship whilst $\Delta > 1$ indicates positive slopes. In the former case, size inequality is more important than species mingling and in the latter case it is the other way round. The sign of the slopes changes approximately at $\Delta \approx 1$ where the relative influence of species and size diversity indices is even (Fig. 6).

Data are nearly always statistically dependent in space and time and spatio-temporal processes can lead to complex interactions (Cressie and Wikle, 2011). This is also likely to be true for data from forest ecosystems and our problem of species community $\bar{M} \sim \bar{T}$ correlation. As part of these complex interactions it is quite possible that spatial and temporal trends differ, since they operate in different dimensions. Commonly, spatial variation in temporal trends is studied but in the case of forest structure, judging by Fig. 6, it is rather a matter of temporal variation in spatial trends: The linear within-plot trends indicated by the orange lines in Fig. 6 are an expression of the temporal variation around the spatial, exponential trend. Although we observed some constancy over time in the $\bar{M} \sim \bar{T}$ community relationship (Fig. 3), there is clearly some limited temporal variation in the $b \sim \Delta$ relationship which we see expressed in the linear within-plot trends.

5. Conclusions

The starting point of active conservation is a comprehensive understanding of how biodiversity including tree diversity is maintained

naturally. The interaction between species and size diversity is crucial to this understanding, since, unlike other plants, trees can come in very different sizes. A consequence of the mingling-size hypothesis usually is that community species mingling and size inequality are positively correlated, i.e. where there is high species mingling in a forest ecosystem, size inequality is high, too. The practical benefit of positive correlations is that it is sufficient for conservation management to monitor and support only spatial species diversity, as size inequality follows suit. However, there is evidence at Knysna Forest that these ecosystems predominantly have negative species mingling \sim size inequality correlations. Negative correlations usually imply that instances of high spatial species mingling are not necessarily related to large trees. In that case high size inequality is not a by-product of high species mingling and conservation management needs to make a special effort to monitor and encourage spatial size inequality in addition to species mingling. Our study has demonstrated that the sign of species mingling \sim size inequality relationships can be inferred from the mark cross correlation function when applying it to the diversity indices of individual trees. We have also learnt that individual-tree size inequality rather than species mingling is mainly responsible for negative community $\bar{M} \sim \bar{T}$ correlations, which is typical of Knysna forest. This type of species-size diversity can practically be maintained as part of active conservation by ensuring a diverse size distribution in each species population, i.e. a wide range of conspecific tree sizes, through selective small-scaled disturbances.

Funding

This research did not receive any specific grant from funding agencies in the public, commercial or non-profit sectors.

CRedit authorship contribution statement

Anna Mariager Behrend: Writing – original draft. **Graham Durheim:** Writing – original draft, Data curation. **Arne Pommerening:**

Writing – original draft, Visualization, Validation, Software, Methodology, Investigation, Formal analysis, Conceptualization.

Declaration of Generative AI and AI-assisted technologies in the writing process

During the preparation of this work the authors did not use any AI or AI-assisted technologies.

Declaration of Competing Interest

The authors declare that they have no known financial interests or personal relationships that could have influenced the work reported in this paper.

Data Availability

Data will be made available on request.

Acknowledgements

GD and AP are grateful to Klaus von Gadow (Göttingen University, Germany) for introducing them to one another and for explaining the data.

References

- Baddeley, A., Rubak, E., Turner, R., 2016. *Spatial Point Patterns. Methodology and Applications with R*. CRC Press, Boca Raton.
- Ballani, F., Pommerening, A., Stoyan, D., 2019. Mark-mark scatterplots improve pattern analysis in spatial plant ecology. *Ecol. Inform.* 49, 13–21.
- Connell, J.H., 1971. On the role of natural enemies in preventing competitive exclusion in some marine animals and in rain forests. In: den Boer, P.J., Gradwell, G.R. (Eds.), *Dynamics of Populations. Centre for Agricultural Publishing and Documentation, Wageningen, the Netherlands.*, pp. 298–312.
- Cressie, N., Wikle, C.K., 2011. *Statistics for spatio-temporal data*. John Wiley & Sons, Hoboken.
- Dale, M.R.T., Fortin, M.-J., 2014. *Spatial analysis. A guide for ecologists*. Second edition. Cambridge University Press, Cambridge.
- Fischer, J., Lindenmayer, D.B., Manning, A.D., 2006. Biodiversity, ecosystem function, and resilience: ten guiding principles for commodity production landscapes. *Front. Ecol. Environ.* 4, 80–86.
- Ford, E.D., 1975. Competition and stand structure in some even-aged plant monocultures. *J. Ecol.* 63, 311–333.
- Gadow, K.V., Zhang, G., Durrheim, G., Drew, D., Seydack, A., 2016. Diversity and production in an Afrotropical Forest. *For. Ecosyst.* 3, 15.
- Gadow, K.V., 1993. Zur Bestandesbeschreibung in der Forsteinrichtung. [New variables for describing stands of trees.] *Forst und Holz* 48, 602–606.
- Hoffmann, S., 2022. Challenges and opportunities of area-based conservation in reaching biodiversity and sustainability goals. *Biodivers. Conserv.* 31, 325–352.
- Hui, G., Hu, Y., Zhao, Z., 2008. Evaluating tree species segregation based on neighbourhood spatial relationships. *J. Beijing For. Univ.* 30, 131–134.
- Hui, G., Zhao, X., Zhao, Z., Gadow, K.V., 2011. Evaluating tree species spatial diversity based on neighborhood relationships. *For. Sci.* 57, 292–300.
- Illian, J., Penttinen, A., Stoyan, H., Stoyan, D., 2008. *Statistical analysis and modelling of spatial point patterns*. John Wiley & Sons, Chichester.
- Janzen, D.H., 1970. Herbivores and the number of tree species in tropical forests. *Am. Nat.* 104, 501–528.
- Kühl, H.S., Bowler, D.E., Bösch, L., Bruehlheide, H., Dauber, J., Eichenberg, D., Eisenhauer, N., Fernández, N., Guerra, C.A., Henle, K., Herbing, I., Isaac, N.J.B., Jansen, F., König-Ries, B., Kühn, I., Nilsen, E.B., Pe'er, G., Richter, A., Schulte, R., Settle, J., van Dam, N.M., Voigt, M., Wägele, W.J., Wirth, C., Bonn, A., 2020. Effective biodiversity monitoring needs a culture of integration. *One Earth* 3, 462–474.
- LeMay, V., Pommerening, A., Marshall, P., 2009. Spatio-temporal structure of multi-storied, multi-aged interior Douglas fir (*Pseudotsuga menziesii* var. *glauca*) stands. *J. Ecol.* 97, 1062–1074.
- Magurran, A.E., 2004. *Measuring biological diversity*. Blackwell Publishing, Oxford. 256p.
- Matias, M.G., Combe, M., Barbera, C., Mouquet, N., 2013. Ecological strategies shape the insurance potential of biodiversity. *Front. Microbiol.* 3, 432.
- McElwee, P., 2021. Climate change and biodiversity loss: two sides of the same coin. *Curr. Hist.* 295–300. November 2021.
- Murphy, S.J., Xu, K., Comita, L.S., 2016. Tree seedling richness, but not neighbourhood composition, influences insect herbivory in a temperate deciduous forest community. *Ecol. Evol.* 6, 6310–6319.
- Ohser, J., Stoyan, D., 1981. On the second-order and orientation analysis of planar stationary point processes. *Biom. J.* 23, 523–533.
- Oliver, T.H., Heard, M.S., Isaac, N.J.B., Roy, D.B., Procter, D., Eigenbrod, F., Freckleton, R., Hector, A., Orme, C.D.L., Petchey, O.L., Proença, V., Raffaelli, D., Suttle, K.B., Mace, G.M., Martín-López, B., Woodcock, B.A., Bullock, J.M., 2015. Biodiversity and resilience of ecosystem functions. *Trends Ecol. Evol.* 30, 673–684.
- Penttinen, A., Stoyan, D., Henttonen, H., 1992. Marked point processes in forest statistics. *For. Sci.* 38, 806–824.
- Pommerening, A., Grabarnik, P., 2019. *Individual-based methods in forest ecology and management*. Springer Nature, Cham.
- Pommerening, A., Stoyan, D., 2006. Edge-correction needs in estimating indices of spatial forest structure. *Can. J. For. Res.* 36, 1723–1739.
- Pommerening, A., Uria-Diez, J., 2017. Do large forest trees tend towards high species mingling? *Ecol. Inform.* 42, 139–147.
- Pommerening, A., LeMay, V., Stoyan, D., 2011. Model-based analysis of the influence of ecological processes on forest point pattern formation – a case study. *Ecol. Model.* 222, 666–678.
- Pommerening, A., Wang, H., Zhao, Z., 2020. Global woodland structure from local interactions: new nearest-neighbour functions for understanding the ontogenesis of global forest structure. *For. Ecosyst.* 7, 22.
- R Development Core Team, 2023. *R: A language and environment for statistical computing*. R Foundation for Statistical Computing, Vienna, Austria. (<http://www.r-project.org>).
- Rajala, T., Illian, J., 2012. A family of spatial biodiversity measures based on graphs. *Environ. Ecol. Stat.* 19, 545–572.
- Román-Palacios, C., Wiens, J.J., 2020. Recent responses to climate change reveal the drivers of species extinction and survival. *Proc. Natl. Acad. Sci. U. S. A.* 117, 4211–4217.
- Seifert, T., Seifert, S., Seydack, A., Durrheim, G., Gadow, K.V., 2014. Competition effects in an afrotemperate forest. *For. Ecosyst.* 1, 13.
- Stoyan, D., 1987. Statistical analysis of spatial point processes: a soft-core model and cross-correlations of marks. *Biom. J.* 29, 971–980.
- Stoyan, D., Penttinen, A., 2000. Recent applications of point process methods in forestry statistics. *Stat. Sci.* 15, 61–78.
- Suzuki, S.N., Kachi, N., Suzuki, J.-I., 2008. Development of local size hierarchy causes regular spacing of trees in an even-aged *Abies* forest: analyses using spatial autocorrelation and the mark correlation function. *Ann. Bot.* 102, 435–441.
- The Royal Society and the US National Academy of Sciences, 2020. *Climate change. Evidence & causes. Update 2020. An overview from the Royal Society and the US National Academy of Sciences. Report*.
- Wang, H., Peng, H., Hui, G., Hu, Y., Zhao, Z., 2018. Large trees are surrounded by more heterospecific neighboring trees in Korean pine broad-leaved natural forests. *Sci. Rep.* 8, 9149.
- Wang, H., Zhang, X., Hu, Y., Pommerening, A., 2021. Spatial patterns of correlation between conspecific species and size diversity in forest ecosystems. *Ecol. Model.* 457, 109678.
- Warton, D.I., Duursma, R.A., Falster, D.S., Taskinen, S., 2012. SMATR 3 – an R package for estimation and inference about allometric lines. *Methods Ecol. Evol.* 3, 257–259.
- Warton, D.I., Wright, I.J., Falster, D.S., Westoby, M., 2006. A review of bivariate line-fitting methods for allometry. *Biol. Rev.* 81, 259–291.
- Weiner, J., Solbrig, O.T., 1984. The meaning and measurement of size hierarchies in plant populations. *Oecologia* 61, 334–336.
- Wills, C., Condit, R., Foster, R.B., Hubbell, S.P., 1997. Strong density- and diversity-related effects help to maintain tree species diversity in a neotropical forest. *Proc. Natl. Acad. Sci. U. S. A.* 94, 1252–1257.
- Yachi, S., Loreau, M., 1999. Biodiversity and ecosystem productivity in a fluctuating environment: the insurance hypothesis. *Proc. Natl. Acad. Sci. U. S. A.* 96, 1463–1468.